

MECHANICAL SCHEMES AND SUSTAINABILITY OF PLASTIC FLOW METAL

Sosenushkin E.H., Yanovskaya E.A., Sosenushkin A.E.

Abstract. Results of the theoretical analysis of invariant criteria for evaluating the stress-strain state under specific mechanical schemes stresses and deformations on forming operations and their impact on the sustainable flow of processes of plastic deformation are presented

Keywords: stress, deformations, invariants tensors, stresses and deformations deviators, sustainability of plastic flow.

1. Introduction.

The shells of various shapes and sizes [1-4] is in high demand due to the development of the energy and chemical engineering, aviation and space industry, valve industry and household appliances. Sheet punching processes [5-7] are the most cost-effective in terms of saving resources and energy. The sheet or tube workpieces may be used as starting material, depending on the necessary operations such as folding sheet and the extractor operations [10.8], distribution and crimping operation [11-14].

Plastic deformation processes are not stationary. Thus, preliminary mathematical [14-16] or computer [17] simulation of applied operations to the assessment of stress-strain state of the metal workpieces with the purpose of forecasting the sustainability of plastic flow are very important.

Deformation scheme differ non-monotonic. Under complex loading deformation direction changes one or more times to the contrary, and there are the fractional deformation processes. Under the terms of continuous medium mechanics [18] for an incompressible material, the deformation of a material point is represented as the trajectory of the radius vector in five-dimensional space of the independent components tensor of deformation. Therefore, under complex loading the trajectory drawn by the end of the radius vector is not smooth with breaks [19] or a smooth but with a curvature. Line length of the loading is a measure of the accumulated deformation at the material point. So there will be the largest value of non-monotonic deformation, because length polyline or smooth curve is bigger than the length of the radius vector. We concluded, if nonmonotonic deformation is implemented for most points in the body, its shape can be changed with a greater degree of deformation. In addition, should be given preference to mechanical deformation schemes dominated shifts [20] when choosing metal forming processes from a number of alternatives. Evaluation of the stress-strain state the deformed metal is the rationale for this choice. It provides a non-monotonic deformation and stable flow forming process at the same time.

2. Preconditions and means for solving the problems

A general idea of stress-strain state can be obtained through O. Mora's pie charts [5-7] for the stresses and deformations. So we have extremity of the principal stresses and the main deformations. Regardless of the selected coordinate system of the stress-strain state is estimated by dimensionless invariant tensor characteristics and / or deviatoric deformations.

The indicator of deformation state schemes (Nadai-Lode's parameter for deformations) [5-7]:

$$V_{\varepsilon} = \frac{2\varepsilon_2 - \varepsilon_1 - \varepsilon_3}{\varepsilon_1 - \varepsilon_3}, \quad (1)$$

where $\varepsilon_1, \varepsilon_2, \varepsilon_3$ the main deformations.

If the indicator takes the value $V_{\varepsilon} = -1$, there will be mechanical deformation schemes with a predominance of extension, at $V_{\varepsilon} = 1$ - there will be mechanical schemes with a pronounced unequal compression and, finally, at $V_{\varepsilon} = 0$ - there will be flat mechanical shift circuits.

According to the criterion of positivity additional loads, plastic flow of an incompressible material is stable until the condition [21]:

$$d\sigma_p \geq \sigma_i d\varepsilon_i. \quad (2)$$

When curve approximation metal hardening power law, we obtain the following expression:

$$\sigma_i = A\varepsilon_i^n, \quad (3)$$

where $A = \sigma_b(1 + \delta)$ - the constant of the metal; $n = \ln(1 + \delta)$ - strain hardening index; δ - a uniform elongation of the sample when it is tested in tension.

This expression can be used to calculate the intensity of deformations accumulated in the process of forming [7, 21]:

$$\frac{\varepsilon_{i\text{kp}}}{n} = \frac{2\sqrt{1 - \alpha + \alpha^2}}{2 - \alpha}, \quad (4)$$

where $\alpha = \frac{\sigma_{\theta}}{\sigma_p}$ - dimensionless parameter of the stress state [7,

21, 22], which is the ratio of the principal stresses.

We pay attention to the axial symmetry of deformation, often encountered in sheet punching forming operations during plastic deformation of shells, and to coaxial principal axes of stress, deformation and deformation rate, and also to the similarity of O.Mora's pie charts for stresses and deformations provided equality indicators of stress and deformation state $V_{\sigma} = V_{\varepsilon}$. Legally, we will use equations relating the stresses and deformations in the form[5, 7, 23]:

$$\frac{\sigma_p - \sigma_{\theta}}{\varepsilon_p - \varepsilon_{\theta}} = \frac{\sigma_{\theta} - \sigma_z}{\varepsilon_{\theta} - \varepsilon_z} = \frac{\sigma_z - \sigma_p}{\varepsilon_z - \varepsilon_p} = \frac{2}{3} \frac{\sigma_i}{\varepsilon_i}, \quad (5)$$

The finite deformation is determined [7, 23]:

$$\varepsilon_p = \ln \frac{d\rho}{dr}; \varepsilon_{\theta} = \ln \frac{\rho}{r}; \varepsilon_z = \ln \frac{s}{s_0}, \quad (6)$$

where r, s_0, ρ, s - accordingly radius and thickness of the selected item in the original and deformed states;

$\varepsilon_i = \sqrt{\frac{4}{3} I_2(D_{\varepsilon})}$ - deformation intensity;

$I_2(D_{\varepsilon})$ - second invariant of the deviatoric of deformations, which represents the amount of deformations, causing plastic forming;

$\sigma_i = \sqrt{3 I_2(D_{\sigma})}$ - stress intensity.

3. Diagram of deformations

In case we projected axis of the coordinate system in which it is built onto the flatness section of the cylinder plasticity deviatoric flatness, we can get the projections of the axes angled

$\frac{2\pi}{3}$ form oblique coordinate system [8-10]. Since the axes stresses and deformations are coaxial. We consider as axes of the main deformation. They are arranged in such a way that for any

point in the flatness with the radius vector incompressibility condition is satisfied:

$$\epsilon_p + \epsilon_\theta + \epsilon_z = 0, \tag{7}$$

where the components of the principal deformations in the trigonometric form are presented as expressions [24]:

$$\begin{aligned} \epsilon_p &= \epsilon_i \cos \varphi_\epsilon; \\ \epsilon_\theta &= \epsilon_i \cos\left(\varphi_\epsilon + \frac{2}{3}\pi\right); \epsilon_z = \epsilon_i \cos\left(\varphi_\epsilon + \frac{4}{3}\pi\right), \end{aligned} \tag{8}$$

and the modulus of the vector $\bar{\epsilon}$ is equal to the intensity of deformations in axisymmetric stress state[25]:

$$|\bar{\epsilon}| = \epsilon_i = \frac{2}{\sqrt{3}} \sqrt{(\epsilon_p - \epsilon_\theta)^2 + (\epsilon_\theta - \epsilon_z)^2 + (\epsilon_z - \epsilon_p)^2} \tag{9}$$

We'll display the deviatoric flatness projection of the principal axes of deformations (Fig. 1).

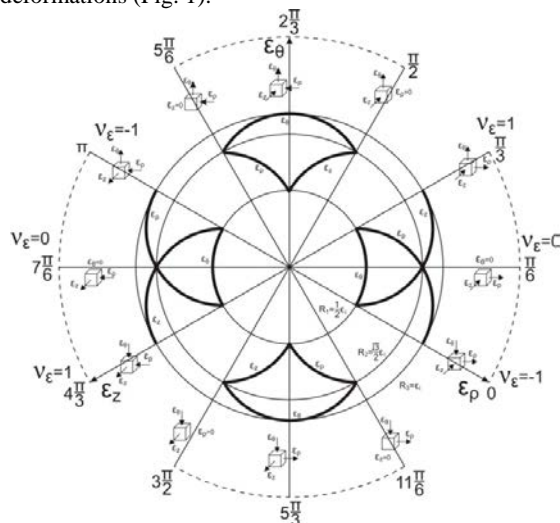


Fig.1. The pie chart of deformations on the deviatoric flatness.

In our case, the projection axis ϵ_p coincides with the direction at the angle $\varphi_\epsilon = 0$ type deformed state, the projection axis ϵ_θ coincides with the direction determined by

the angle $\varphi_\epsilon = \frac{2\pi}{3}$, and the projection axis ϵ_z coincides with

the direction at the angle $\varphi_\epsilon = \frac{4\pi}{3}$. We draw concentric circles

with centers located at the origin and with radius accordingly

$R_1 = \frac{1}{2}\epsilon_i$; $R_2 = \frac{\sqrt{3}}{2}\epsilon_i$; $R_3 = \epsilon_i$, where ϵ_i is taken as the

scale factor. Except projections of the principal axes in the chart

we choose the direction of steps in the angle $\Delta\varphi_\epsilon = \frac{\pi}{6}$ in the

range $0 \leq \varphi_\epsilon \leq 2\pi$ additionally. In Table. 1 we show the results of calculating of the main deformations by (8) for each value of the angle type deformed state.

Table 1. Values of the principal deformation and strain state indicator

φ_ϵ	0	$\frac{\pi}{6}$	$\frac{\pi}{3}$	$\frac{\pi}{2}$	$\frac{2\pi}{3}$	$\frac{5\pi}{6}$	π	$\frac{7\pi}{6}$	$\frac{4\pi}{3}$	$\frac{3\pi}{2}$	$\frac{5\pi}{3}$	$\frac{11\pi}{6}$
ϵ_p	ϵ_i	$\frac{\sqrt{3}}{2}\epsilon_i$	$\frac{1}{2}\epsilon_i$	0	$-\frac{1}{2}\epsilon_i$	$-\frac{\sqrt{3}}{2}\epsilon_i$	$-\epsilon_i$	$-\frac{\sqrt{3}}{2}\epsilon_i$	$-\frac{1}{2}\epsilon_i$	0	$\frac{1}{2}\epsilon_i$	$\frac{\sqrt{3}}{2}\epsilon_i$
ϵ_θ	$-\frac{1}{2}\epsilon_i$	0	$\frac{1}{2}\epsilon_i$	$\frac{\sqrt{3}}{2}\epsilon_i$	ϵ_i	$\frac{\sqrt{3}}{2}\epsilon_i$	$\frac{1}{2}\epsilon_i$	0	$-\frac{1}{2}\epsilon_i$	$-\frac{\sqrt{3}}{2}\epsilon_i$	$-\epsilon_i$	$-\frac{\sqrt{3}}{2}\epsilon_i$
ϵ_z	$-\frac{1}{2}\epsilon_i$	$-\frac{\sqrt{3}}{2}\epsilon_i$	$-\epsilon_i$	$-\frac{\sqrt{3}}{2}\epsilon_i$	$-\frac{1}{2}\epsilon_i$	0	$\frac{1}{2}\epsilon_i$	$\frac{\sqrt{3}}{2}\epsilon_i$	ϵ_i	$\frac{\sqrt{3}}{2}\epsilon_i$	$\frac{1}{2}\epsilon_i$	0
V_ϵ	-1	0	1				-1	0	1			

We chose the values of the principal deformations in the form of points on the appropriate direction and we joined them congruent circular arcs with radius R_1 . We obtain a deformation path of a star whose curvature says nonmonotonicities deformation processes (see Fig. 1).

In addition, each direction is uniquely characterized by mechanical deformation scheme. Mechanical shifter schemes are realized at directions for angles $\frac{\pi}{6}$ and $\frac{7\pi}{6}$ of the form of the deformed state. Analysis shows that in addition the mechanical

shifter scheme is realized at the corners $\frac{\pi}{2}$, $\frac{5\pi}{6}$, $\frac{3\pi}{2}$, $\frac{11\pi}{6}$ of

the form of the deformed state. This means that the Nadai-Lode's parameter for deformations in these directions should be equal.

$v_\epsilon = 0$.

Curvature of the trajectories deformation allows to assert nonmonotonicity of deformation in the implementation of these stamping operations.

4. Rigidity of scheme of stress state

We define the value of the indicator of scheme stiffness stress. Here we used G.D. Dheli's technique [22]. The only difference is that we consider more general axisymmetric stress-strain state instead of flat.

From the incompressibility condition (7) and the values of finite deformations (6) termwise differentiation we'll have:

$$\rho \frac{d\varepsilon_\theta}{d\rho} = 1 - e^{\varepsilon_z} \cdot e^{2\varepsilon_\theta} \quad (10)$$

After integrating the resulting differential equation:

$$e^{-2\varepsilon_\theta} = e^{\varepsilon_z} + \frac{c}{\rho^2}.$$

Taking the logarithm we obtain the expression

$$\varepsilon_\theta = -\frac{1}{2} \ln \left(e^{\varepsilon_z} + \frac{c}{\rho^2} \right). \quad (11)$$

We define the constant of integration of the boundary conditions $\rho = r_k$ for deformation $\varepsilon_\theta = \tilde{\varepsilon}_\theta = \ln \frac{r_k}{r}$.

$$\tilde{\varepsilon}_\theta = -\frac{1}{2} \ln \left(e^{\varepsilon_z} + \frac{c}{r_k^2} \right).$$

Potential gives us

$$e^{-2\varepsilon_\theta} = e^{\varepsilon_z} + \frac{c}{r_k^2}, \text{ whence } c = r_k^2 (e^{-2\tilde{\varepsilon}_\theta} - e^{\varepsilon_z}).$$

We substitute the expression in (15):

$$\varepsilon_\theta = -\frac{1}{2} \ln \left[e^{\varepsilon_z} + \frac{r_k^2}{\rho^2} (e^{-2\tilde{\varepsilon}_\theta} - e^{\varepsilon_z}) \right]. \quad (12)$$

Constraint equations stresses and deformations (5) we can see

the validity of the expression: $\sigma_\theta = \sigma_{cp} + \frac{2}{3} \sigma_i \frac{\varepsilon_\theta}{\varepsilon_i}$;

(13)

where $\sigma_{cp} = \frac{\sigma_1 + \sigma_2 + \sigma_3}{3}$ - average normal stress. If

$\sigma_{cp} > 0$, diagram of the stress state is tough.

Under the condition of incompressibility $\varepsilon_\rho = -\varepsilon_\theta - \varepsilon_z$

equation (9) takes the form $\varepsilon_i = \frac{2}{\sqrt{3}} \sqrt{\varepsilon_\theta^2 + \varepsilon_\theta \varepsilon_z + \varepsilon_z^2}$. A

deformable shell wall thickness $\varepsilon_i = \frac{2}{\sqrt{3}} \varepsilon_\theta$ is constant, so

$$\varepsilon_i = \frac{1}{\sqrt{3}} \ln \left[e^{\varepsilon_z} + \frac{r_k^2}{\rho^2} (e^{-2\tilde{\varepsilon}_\theta} - e^{\varepsilon_z}) \right]. \quad (14)$$

We represent (13) as follows:

$$\sigma_\theta = \frac{\sigma_i \left(\frac{3\sigma_{cp}}{\sigma_i} \varepsilon_i + 2\varepsilon_\theta \right)}{3\varepsilon_i}. \quad (15)$$

Expression indication of the stiffness scheme stress state [5, 7, 20, 21] is:

$$\eta = \frac{3\sigma_{cp}}{\sigma_i} \quad (16)$$

We substitute in (15) and taking into account (12) and (14) we obtain the dependence of normal stress σ_θ :

$$\sigma_\theta = \frac{\sigma_i}{3} (\eta + \sqrt{3}). \quad (17)$$

Doing the same actions, we define the normal stress σ_ρ :

$$\sigma_\rho = \frac{\sigma_i}{3} (\eta - \sqrt{3}). \quad (18)$$

Differential equation of equilibrium in the form of an axisymmetric shell deformation with friction [5-7]:

$$\rho \frac{d\sigma_\rho}{d\rho} + \sigma_\rho - \sigma_\theta - \frac{\mu\rho}{\sin \alpha} \left(\frac{\sigma_\rho}{R_\rho} + \frac{\sigma_\theta}{R_\theta} \right) = 0. \quad (19)$$

If stamped shell is conical, the differential equation of

equilibrium is simplified $\rho \frac{d\sigma_\rho}{d\rho} + \sigma_\rho - \sigma_\theta (1 + \mu ctg \alpha) = 0$.

(20)

We substitute the values of the principal stresses (17) and (18) in the differential equation of equilibrium (20):

$$\rho \frac{d \left[\frac{\sigma_i}{3} (\eta - \sqrt{3}) \right]}{d\rho} + \frac{\sigma_i}{3} (\eta - \sqrt{3}) - \frac{\sigma_i}{3} (\eta + \sqrt{3}) (\mu ctg \alpha) = 0$$

Some transformations lead to a differential equation with separable variables:

$$\rho \frac{d\eta}{d\rho} = \eta \mu ctg \alpha + \sqrt{3} (\mu ctg \alpha + 2). \quad (21)$$

After integrating the resulting equation will be:

$$\ln [\eta \mu ctg \alpha + \sqrt{3} (\mu ctg \alpha + 2)] = \ln [(c\rho)^{\mu ctg \alpha}] \quad (22)$$

The conditions at $\rho = r_0$ $\eta = 0$ are boundary to determine the constant of integration:

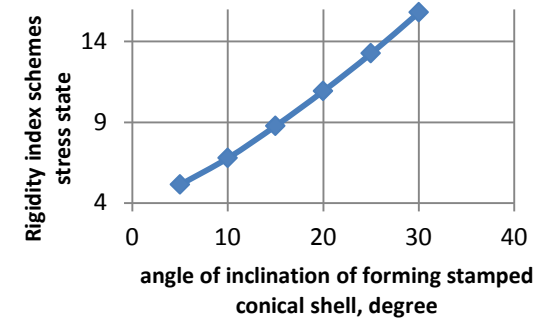
$$c = \frac{1}{r_0} \left[\sqrt{3} (\mu ctg \alpha + 2) \right]^{\frac{1}{\mu ctg \alpha}}. \quad (23)$$

After substituting the constant of integration and the necessary transformations, we find the expression for determining stiffness index of scheme stress state:

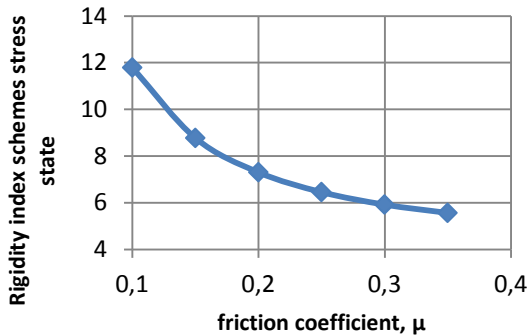
$$\eta = \frac{\sqrt{3} (\mu ctg \alpha + 2)}{\mu ctg \alpha} \left[\left(\frac{\rho}{r_0} \right)^{\mu ctg \alpha} - 1 \right]. \quad (24)$$

5. Results of calculation of the indicator.

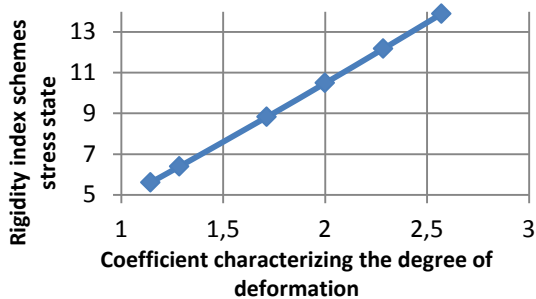
We consider forming a conical tube using a tool as an example evaluation of deformability Fig. 2 illustrates a change rigidity index in the stress state scheme depending on the taper angle of stamped shell (a) from the friction coefficient μ (b) and from a coefficient characterizing the extent of the deformation (c).



a)



b)



c)

Fig. 2. The change in the rigidity index schemes of the stress state of scheme: a - angle of inclination of forming stamped conical shell, b - the friction coefficient; c - the coefficient characterizing the degree of deformation.

Obviously, when the taper angle of forming of stamped shell is increasing, rigidity index of scheme of stress state η increases. Rigidity index makes the stress state more rigid and similarly it affects to the value η of and the coefficient characterizing the degree of deformation, the higher it is, the harder the scheme of stress will be.

An increase of coefficient of friction μ makes the scheme of stress state less rigid. It confirms the well-known in practice position that at lower values of the friction coefficient the ability to localize stresses increases. It inevitably leads to the neck formation and further destruction of the boundary wall of of stamped parts.

Therefore, the rigidity index of the stress state, along with other invariant characteristics may be an estimate of the stability of plastic flow processes.

Literature.

1. Артес А.Э., Сосенушкин Е.Н. Проблемы производства крупных поковок в отечественном машиностроении. // Справочник. Инженерный журнал с приложением. – 2012. - №9. – С.45-50.
2. Сосенушкин Е.Н. Ресурсосберегающие технологии изготовления деталей трубопроводной арматуры. // Технология машиностроения. – 2010. - №3. – С.14-16.
3. Сосенушкин Е.Н., Третьюхин В.В., Яновская Е.А. Технологические процессы штамповки изделий из толстостенных труб// Кузнечно-штамповочное производство. Обработка металлов давлением. – 2013.-№2.- С.25-29.

4. Сосенушкин Е.Н., Климов В.Н., Яновская Е.А. Кутышкина Е.А. Экспериментальные исследования формоизменения стальных труб.// Кузнечно-штамповочное производство. Обработка металлов давлением. – 2010. – №6. – С.39-43.

5. Теория обработки металлов давлением: учебник для вузов./ Голенков В.А., Яковлев С.П., Головин С.А. [и др.]. – М.: Машиностроение, 2013. – 442 с.

6. Сторожев М.В., Попов Е.А. Теория обработки металлов давлением. –М.: Машиностроение, 1977. - 423 с.

7. Томленов А.Д. Теория пластического деформирования металлов./ А.Д. Томленов. – М.: Металлургия, 1972. – 408 с.

8. Назарян Э.А., Константинов В.Ф. Кинематика деформирования в формоизменяющих операциях листовой штамповки// Вестник машиностроения. – 1999. – №2. – С.35-41.

9. Назарян Э.А., Араб Н.Н. Деформации при отбортовке круглых отверстий в тонких пластинах. // Заготовительные производства в машиностроении. – 2009. - №3. – С.22-26.

10. Назарян Э.А., Аракелян М.М. Предельное формоизменение при деформировании осесимметричных оболочек.// Заготовительные производства в машиностроении. – 2004. - №5. – С.24-27.

11. Сосенушкин Е.Н., Артес А.Э., Яновская Е.А., Хачатрян Д.В. Трубные заготовки: технологический аспект раздачи и обжима. // Вестник МГТУ «Станкин». 2010. №4(12). – С.36-41.

12. Пономарев А.С., Сосенушкин Е.Н., Климов В.Н. Влияние технологических особенностей обработки давлением на микроструктуру и качество деталей трубопроводной арматуры из высокопрочного чугуна.//

13. Сосенушкин Е.Н., Яновская Е.А., Хачатрян Д.В., Киндеров В.Ю. Теоретические и технологические аспекты обжима трубных заготовок.// Известия МГТУ «МАМИ». -№2.- 2013.-г.2. – С.139-145.

14. Сосенушкин Е.Н., Смолович И.Е., Яновская Е.А., Хачатрян Д.В., Киндеров В.Ю. Математические модели операций раздачи и обжима при формообразовании конических участков труб.// Проблемы машиностроения и автоматизации. – 2013. - №4.- С.80-88.

15. Napershin R.I. Pressing a rigid-plastic strip through a curvilinear matrix channel // Mechanics of Solids. - 2008. - Т. 43, № 2. - С. 300-313.

16. Сосенушкин Е.Н., Яновская Е.А., Хачатрян Д.В., Смолович И.Е., Киндеров В.Ю. Моделирование операции раздачи трубных заготовок// Известия ТулГУ. Технические науки. – 2013. – Вып.3. – С.618-631.

17. Сосенушкин Е.Н., Артес А.Э., Третьюхин В.В., Махдиян А. Групповые технологические процессы штамповки трубных переходов в мелкосерийном и серийном производстве.// Кузнечно-штамповочное производство. Обработка металлов давлением. – №7. – 2007. – С.18–24.

18. Ильюшин А.А. Механика сплошной среды. - М.: Изд. Моск. ун-та, 1978. – 287 с.

19. Утяшев Ф.З. Современные методы интенсивной пластической деформации. – Уфа: УГАТУ, 2008. – 313 с.

20. Ганаго О.А., Шестаков Н.А. О показателях эффективности процессов пластического деформирования.// Кузнечно-штамповочное производство. – 1986. - №10. – С.3-4.

21. Ренне И.П., Грдилян Г.Л., Зиновьев В.С. Устойчивость пластического течения в процессах формообразования листовых заготовок из трансверсально-изотропного материала.// Кузнечно-штамповочное производство. – 1978. - №3. – С.17-21.

22. Дель Г.Д. Технологическая механика. – М.: Машиностроение, 1978. – 175 с.

23. Смирнов-Аляев Г.А. Сопротивление материалов пластическим деформациям. – Л.: Машгиз, 1949. – 248 с.

24. Малинин Н.Н. Прикладная теория пластичности и ползучести. – М.: Машиностроение, 1968. – 400 с.

25. Колмогоров В.Л. Механика обработки металлов давлением. – М.: Машиностроение, 1986. – 688 с.